Light-responsive Smart Nanopaper and Ink: Design for Information Storage and Encryption

Zhao Zhang [a], Xiena Kang [a], Xinyu Zhao [a, *], Xiaomin Dai [b], Xiaolin Su [a], Boying Yang [a], Yuxia Luo [a], Chuanyin Xiong [a], Hui Chang [c], Xinping Li [a, *]

[a] *College of Bioresources Chemical and Materials Engineering, Shaanxi University of Science and Technology, Xi'an 710021, Shaanxi, P. R. China.*

[b] *School of Chemistry and Chemical Engineering, Yulin University, Yulin 719000, Shaanxi, P. R. China.*

[c] *College of Mechanical and Electrical Engineering, Shaanxi University of Science and Technology, Wude Road, Weiyang District, Xi'an 710021, P. R. China.*

** To whom correspondence should be addressed:*

E-mail: lixp@sust.edu.cn; 210111075@sust.edu.cn

Reagents and Materials

All chemicals were used as received without any further purification. N,N-dimethylformamide (DMF，99.5%) and ethanol (are analytical reagents, purchased from Damao Reagent Co., Ltd. (Tianjin, China). Rare earth compounds include Terbium trichloride hexahydrate [$TbCl_3 \cdot 6H_2O$ (99.9%)] and Europium trichloride hexahydrate [$EuCl_3 \cdot 6H_2O$ (99.9%)], PEG (molecular weight: 20000), 1-(2-hydroxyethyl)-3,3-dimethylindoline-6'-nitrobenzo Spiropyrans (SP), Poly(vinyl alcohol) 1788 (PVA) and 1,3,5-benzenetricarboxylicacid (98%) were purchased from Aladdin Reagent Co., Ltd. During the experiment, deionized water was self-made by the laboratory. PU touch photosensitive oil was purchased from Xinle Printing Equipment Co., Ltd. (Dongguan, China). The laboratory

softwood bleached kraft pulp is used as the raw material, and the nano cellulose filament is prepared by the high-pressure homogenization process. And all the coordination polymers were acquired in a Teflon-lined stainless steel vessel under autogenous pressure and then slowly cooled down to room temperature.

Characterization

The surface morphology and of the nanopapers and Tb-MOFs were examined using scanning electron microscopy (SEM, JEOL, and Japan) instrumentation. The uniformity of element distribution was obtained through energy dispersive spectrometer (JEOL, and Japan) testing. The uniformity of element distribution was obtained through energy dispersive spectrometer (JEOL, and Japan) testing. Fourier transform infrared spectroscopy (FT-IR, VECTOR-22, Bruker Company, Germany) was recorded in the spectral range from 4000 to 400 cm^{-1} (The solid samples were characterized by KBr particle method and ATR excipients were applied to nanopapers). UV-vis spectra (200-800 nm) were recorded using a Cary 5000 by UV spectrophotometer (UV-VIS, PerkinElmer, USA). XRD analyses were investigated by an X-ray diffractometer (XRD, D8 Advance, Bruker Company, Germany). Stress−strain curves of the nanopapers were obtained using Servo material multifunctional high and low temperature control testing machine (CMT6503, Shenzhen, SANS Test Machine Co. Ltd.). The anti-fatigue performance of the photochromic nanoparticles was determined by UV spectrophotometer (UV-VIS, PerkinElmer, USA). The distribution of fluorescent dots on the surface of Ln-photoetchable nanopapers, Ln-inks was examined using laser scanning confocal microsmcopy (LSCM, LSM800, Carl Zeiss, Germany). The photoluminescence (PL) spectrum was measured with a fluorospectro photometer (FS5, Edinburgh, US). TG and DTG

analyses of the test materials were obtained using an SDTQ600 apparatus under a nitrogen atmosphere at a low rate of 100 mL•min−1. DSC experiments of the experimental samples were conducted using a DSC 200 F3 apparatus; the heating rate was 5 °C/min (35~800 °C). The water contact angle of the Ln-PU-ink were measured using a video optical contact angle (OCA 20, German dataphysics). The gas adsorption capacity of Ln-MOFs and Ln-MOFs @ SP was measured by Brunauer-Emmett-Teller (BET)-physical adsorption instrument (SAP2460 sn:506). The ultraviolet lamp (45 W) and white light lamp (20 W) was purchased from Shanghai Jingke Industrial Co., Ltd. and Shenzhen Jiahua Color Electronics Co., Ltd., respectively.

Figure S1. PXRD spectrum of Pure nanopaper, Tb-nanopaper@SP, and 1:16-nanaopaper@SP.

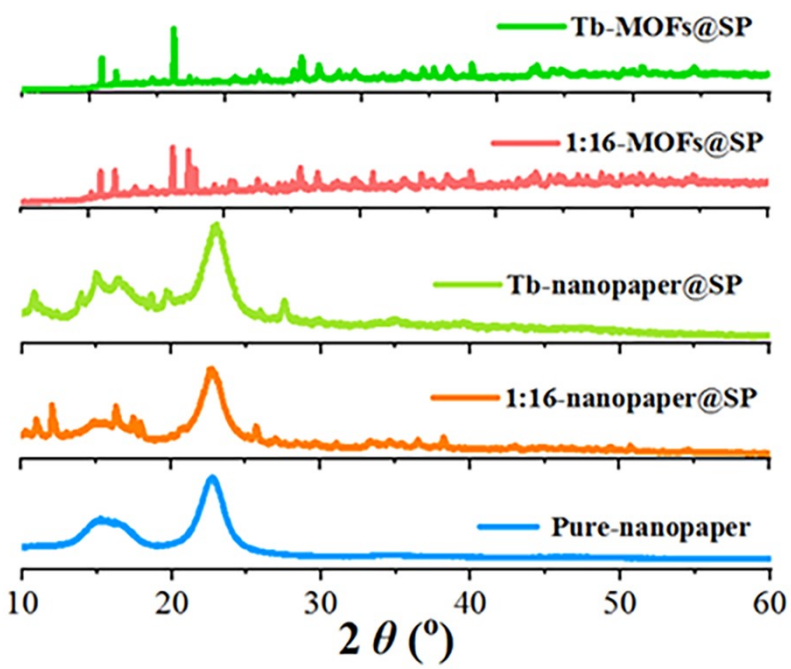

Figure S2. FT-IR spectrum of Ln-MOFs and Ln-MOFs@SP (Ln = Eu, Tb, and 1:16).

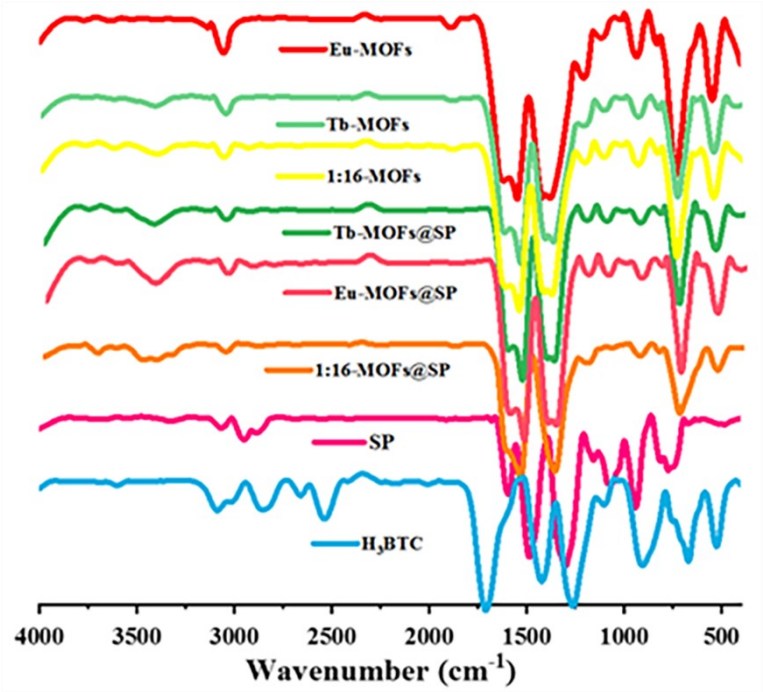

Figure S3. FT-IR spectrum of pure nanopaper, Tb-nanopapers@SP and 1:16-nanopaper@SP.

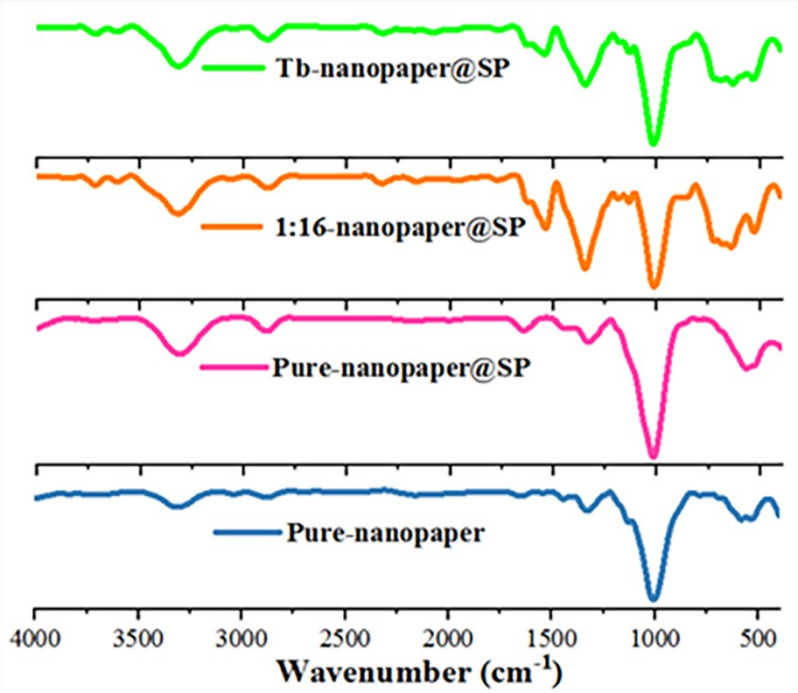

Figure S4. SEM spectrum of Tb-nanopaper (left); EDS spectrum of CNFs of Tb (right)

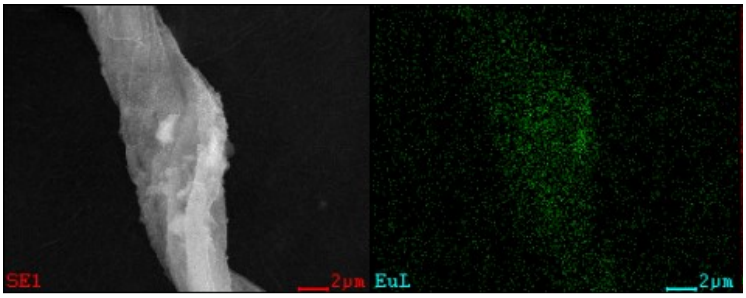

Figure S5. SEM surface image of Tb-nanopaper@SP (a); SEM cross-section image of Tb-nanopaper@SP (b); SEM surface image of Pure-nanopaper (c); SEM cross-section image of Pure-nanopaper (d).

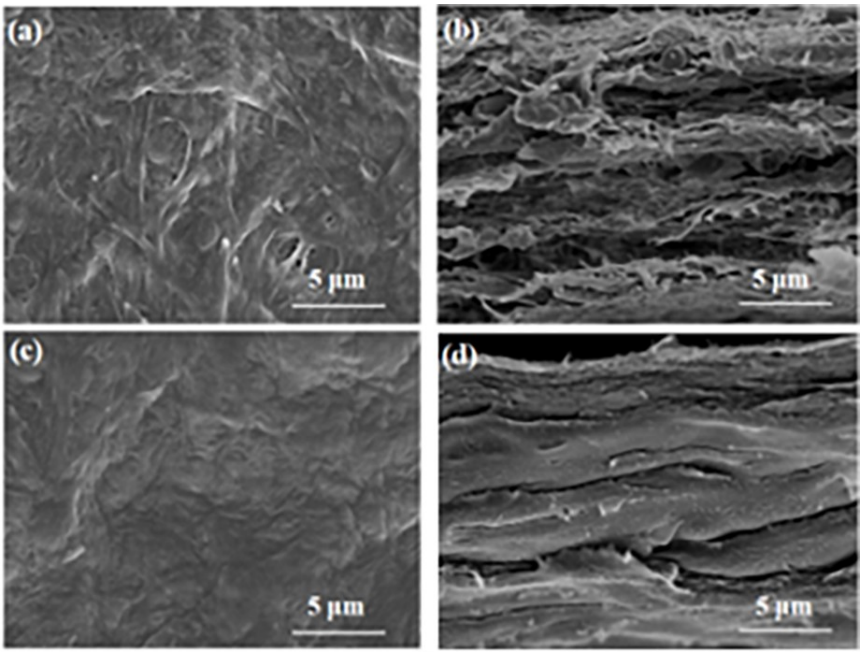

Figure S6. UV-vis absorption spectra of Ln-MOFs, Ln-MOFs@SP and Ln-nanopaper@SP (Ln = Eu or Tb).

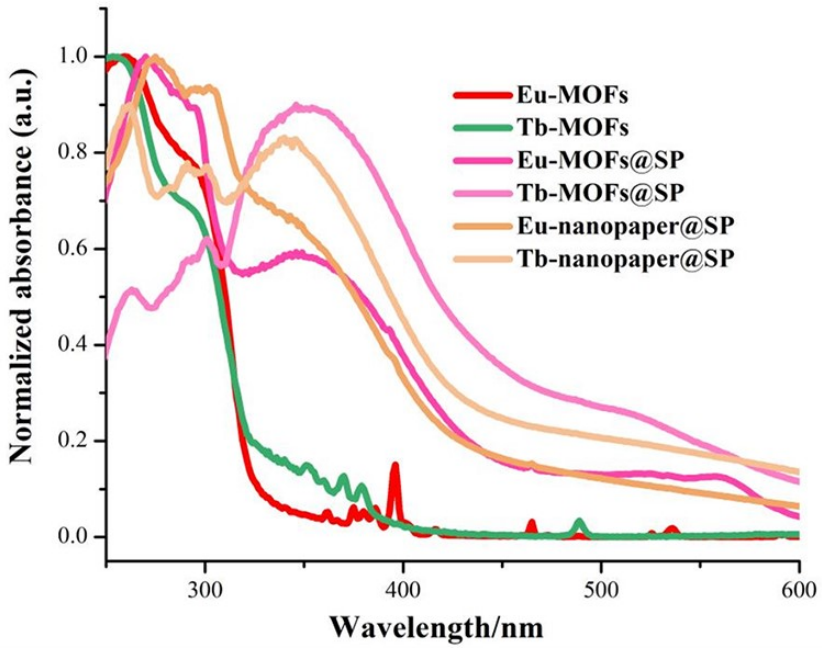

Figure S7. UV-vis absorption spectra of Ln-MOFs@MC and Ln-nanopaper@MC (Ln = Eu or Tb).

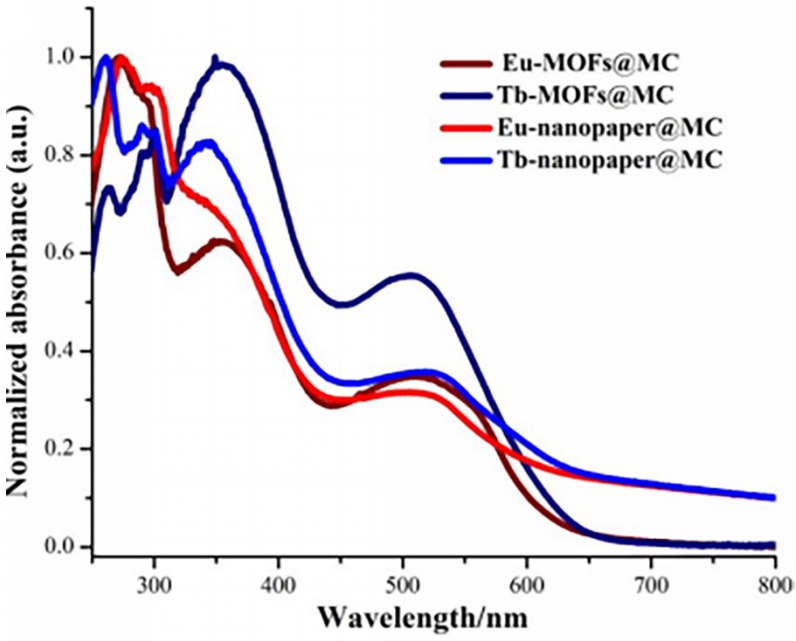

Figure S8. Emission spectra of Eu-MOFs@SP, Tb-MOFs@SP, Eu/Tb = 1/16-MOFs@SP excitation at 396nm.

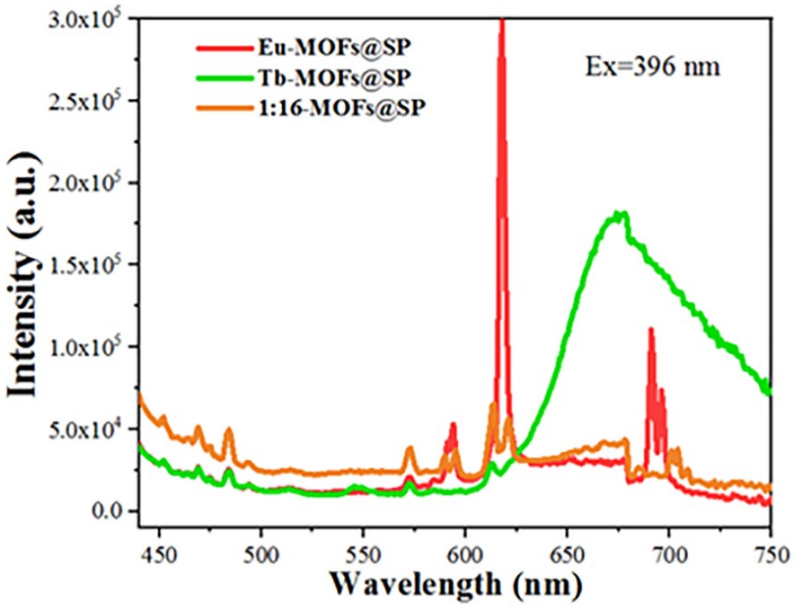

Figure S9. CIE coordinates of Eu-MOFs@SP, Tb-MOFs@SP, Eu/Tb = 1/16-MOFs@SP excitation at 297nm. Eu-MOFs@SP (x=0.390，y=0.342); Tb-MOFs@SP (x=0.409, y=516); 1:16-MOFs (x=0.576, y=0.345).

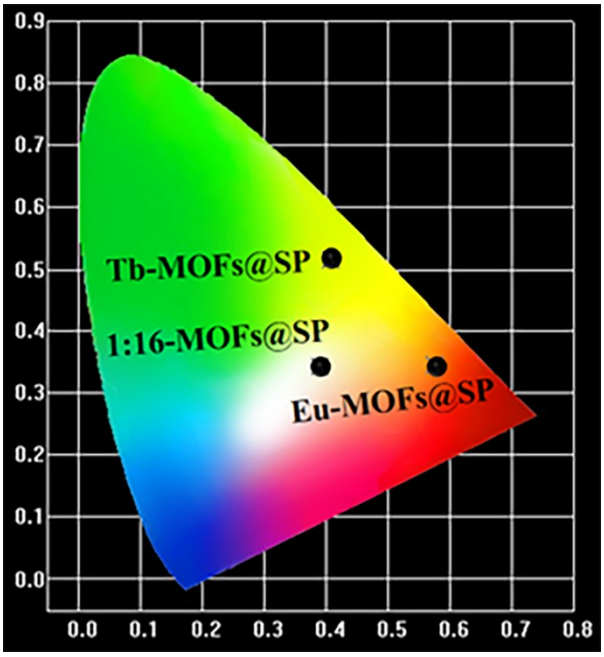

Figure S10. CIE coordinates of Eu-MOFs@SP, Tb-MOFs@SP, Eu/Tb = 1/16-MOFs@SP excitation at 396 nm. Eu-MOFs@SP(x=0.456，y=0.296)；Tb-MOFs@SP(x=0.488，y=0.221)； 1:16-MOFs@SP(x=0.325， y=0.251).

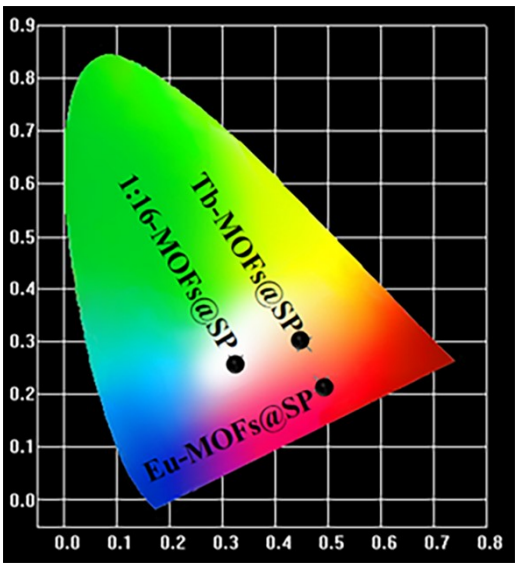

Figure S11. Emission spectra of Eu-nanopaper@SP, Tb-nanopaper@SP, 1:16-nanopaper@SP excited at 396 nm.

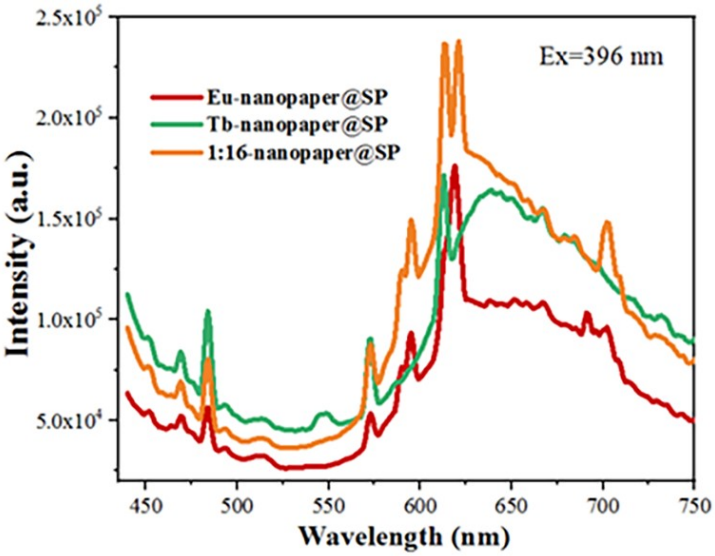

Figure S12. CIE coordinates of Eu-nanopaper@SP, Tb-nanopaper@SP, 1:16-nanopaper@SP excitation at 396nm. Eu-nanopaper@SP (x=0.465 y=0.319)；Tb-nanopaper@SP (x=0.437, y=0.302)；1:16-nanopaper@SP (x=0.516, y=0.312).

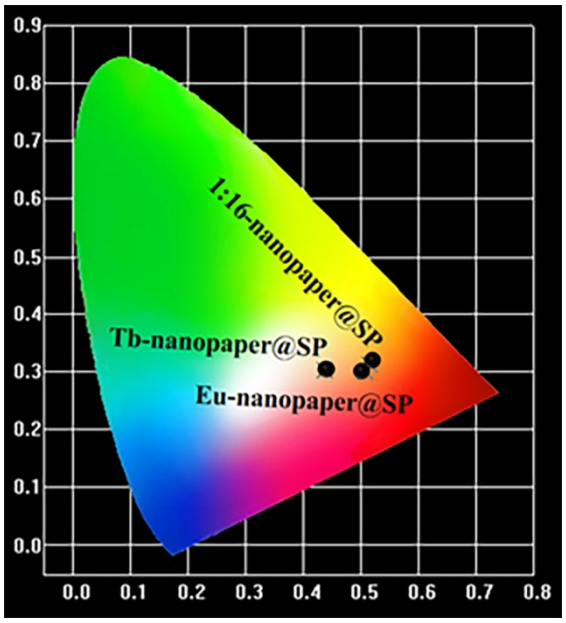

Figure S13. Optical stability of Tb-nanopaper@SP